

Development and Test of a Single-Aperture 11 T Nb₃Sn Demonstrator Dipole for LHC Upgrades

A.V. Zlobin, N. Andreev, G. Apollinari, B. Auchmann, E. Barzi, R. Bossert, G. Chlachidze, M. Karppinen, F. Nobrega, I. Novitski, L. Rossi, D. Smekens, D. Turrioni, R. Yamada

Abstract—The upgrade of the LHC collimation system expects installation of additional collimators in the dispersion suppressor areas around the LHC ring. The longitudinal space for the collimators could be provided by replacing some 8.33 T Nb-Ti LHC main dipoles with shorter 11 T Nb₃Sn dipoles compatible with the LHC lattice and main systems. To demonstrate this possibility FNAL and CERN have started a joint program with the goal of building a 5.5 m long twin-aperture dipole prototype suitable for installation in the LHC. The first step of this program is the development of a 2 m long single-aperture demonstrator dipole with the nominal field of 11 T at the LHC nominal current of 11.85 kA and 60 mm bore with ~20% margin. This paper describes the design, construction and test results of the first single-aperture Nb₃Sn demonstrator dipole model.

Index Terms— Superconducting accelerator magnet, LHC collimation system, demonstrator, magnet test.

I. INTRODUCTION

THE LHC operation plans include an upgrade of the LHC collimation system [1]. Additional cold collimators will be installed in the dispersion suppression (DS) around points 2, 3 and 7, and high luminosity interaction regions at points 1 and 5. The required space of ~3.5 m for the additional collimators could be provided by using 11 T dipoles as a replacement for several 8.33 T LHC main dipoles (MB). These dipoles, operating at 1.9 K and powered in series with the MB's, will deliver the same integrated strength at the nominal LHC current. The operation field level requires using Nb₃Sn superconductor. Recent advances in the development of high-field Nb₃Sn accelerator magnets suggest that this technology is practically ready for this application.

To demonstrate feasibility, CERN and FNAL have started a R&D program to build and test a 5.5 m long twin-aperture Nb₃Sn dipole for the LHC upgrade. Two such cold masses with a cold collimator in between will replace one 14.3 m long LHC MB dipole. The program started in 2011 with the design and construction of a 2 m long single-aperture Nb₃Sn demonstrator dipole magnet with a 60 mm bore, an 11 T field at the LHC nominal current of 11.85 kA and 20% margin [2].

Manuscript received October 9, 2012. Work supported by Fermi Research Alliance, LLC, under contract No. DE-AC02-07CH11359 with the U.S. Department of Energy and European Commission under FP7 project HiLumi LHC, GA no.284404.

N. Andreev, G. Apollinari, E. Barzi, R. Bossert, G. Chlachidze, F. Nobrega, I. Novitski, D. Turrioni, A.V. Zlobin are with Fermi National Accelerator Laboratory, P.O. Box 500, Batavia, IL 60510, USA (phone: 630-840-8192; fax: 630-840-8079; e-mail: zlobin@fnal.gov).

B. Auchmann, M. Karppinen, L. Rossi, D. Smekens are with the European Organization for Nuclear Research, CERN CH-1211, Genève 23, Switzerland.

This paper summarizes the design and assembly details of the single-aperture Nb₃Sn demonstrator dipole and discuss its quench performance. Results of magnetic measurements and heater study are reported elsewhere [3, 4].

II. MAGNET DESIGN

The design concept of the single-aperture 11 T Nb₃Sn demonstrator dipole is described in [5]. To adapt the beam sagitta in straight 11 m long Nb₃Sn magnets, the coil aperture was increased to 60 mm. The coil cross-section was optimized to provide a dipole field of 11 T at the 11.85 kA current with 20% margin, and geometrical field errors below the 10⁻⁴ level.

The coil cross-section was designed using 15.1 mm wide and 1.29 mm thick Rutherford cable and 0.10 mm thick insulation. The 6-block coil consists of 22 turns in the inner layer and 34 turns in the outer layer separated by the 0.506 mm thick interlayer insulation. The mid-plane insulation is 0.125 mm per coil. Coil end blocks were designed to reduce the field level and minimize integrated low-order field harmonics.

The cross-section of the demonstrator dipole cold mass is shown in Fig. 1. Coil pre-stress and support is provided by stainless steel collars, a vertically split iron yoke, Aluminium clamps and a thick stainless steel skin. Two thick stainless steel end plates restrict the axial coil motion.

The coil pre-stress has to be sufficient to compensate for the differences in the coil and structure thermal contractions during cool-down, and for the Lorentz forces during magnet excitation. The design of the mechanical structure and the coil pre-stress were optimized to maintain the coils under compression up to the maximum design field of 12 T and keep the coil stress below 165 MPa during magnet assembly and operation.

Magnet quench protection is provided by internal strip heaters installed between the ground insulation layers.

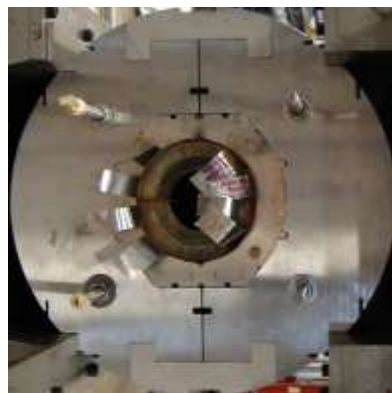


Fig. 1. Cross-sections of the cold mass.

III. MAGNET CONSTRUCTION

The details of the demonstrator dipole construction are reported in [6].

A. Strand and cable

The cable was made of Nb₃Sn RRP-108/127 strand with $D_{eff} \sim 55 \mu\text{m}$, the nominal $J_c(12T, 4.2K) \sim 2750 \text{ A/mm}^2$, the Cu fraction ~ 0.53 and $RRR > 60$ [7]. The Rutherford cable has 40 Nb₃Sn strands 0.7 mm in diameter, a 15 degree transposition angle and an 85% packing factor. The I_c degradation after cabling based on the extracted strand tests is $\sim 4\%$ [8].

A 440 m long piece of cable was fabricated at FNAL providing two ~ 200 m long unit lengths for the demonstrator dipole coils and ~ 25 m piece for short sample measurements. The cable was made in two steps, first, with rectangular cross-section and then, after annealing, it was re-rolled into the final keystone cross-section (Fig. 2). A ~ 220 m cable piece for a spare coil was fabricated at CERN using a one step procedure.



Fig. 2. Keystone 40-strand cable.

B. Coils, ground insulation, quench heaters

Each coil consists of two layers, 6 blocks and 56 turns. Both layers were wound from a single piece of cable insulated with two layers of 0.075 mm thick and 12.7 mm wide E-glass tape. The coil poles were made of Ti-6Al-4V alloy and wedges of stainless steel. The end spacers were also made of stainless steel using the selective laser sintering (SLS) process. The cable layer jump is integrated into the lead end spacers.

Coils were made using the wind-and-react method. During winding each coil layer was impregnated with CTD1202x liquid ceramic binder and cured under a small pressure at 150°C for 0.5 hour. During curing the coil layers were shimmed azimuthally to the same size of 1 mm smaller than the nominal coil size to prevent turn over-compression due to expansion of the Nb₃Sn cable during reaction [9]. Each coil was reacted separately in Argon using a 3-step cycle with $T_{max} = 640^\circ\text{C}$ for 48 hours. Coil pictures after curing and reaction are shown in Fig. 3.

Before impregnation the Nb₃Sn coil leads were spliced to flexible Nb-Ti cables and the coil was wrapped with a 0.125 mm thick layer of E-glass cloth. Coils were impregnated with CTD101K epoxy and cured at 125°C for 21 hours. The radial and azimuthal coil sizes were controlled in the free condition using 3D Cordax machine. The length of two coils, MBH02 and MBH03, used in the demonstrator dipole was 1965 and 1971 mm respectively including coil saddles and splice box.



Fig. 3. Coil after curing (left) and reaction (right).



Fig. 5. Assembly of two coils with quench heaters and ground insulation (left) and collar block installation (right).

The coil ground insulation consists of 5 layers of 0.125 mm thick Kapton film. Two quench protection heaters composed of 0.025 mm thick stainless steel strips were installed on each side of the coil. One heater was placed between the 1st and 2nd Kapton layers and the other one between the 2nd and 3rd layers, covering the outer-layer coil blocks. The corresponding strips on each side of each coil were connected in series forming two independent heaters.

C. Magnet Assembly and instrumentation

Two coils surrounded by the ground insulation and 316L stainless steel protection shells were placed inside the laminated collars made of Nirossta High-Mn stainless steel. Assembly of two coils with quench heaters and ground insulation and collar block installation are shown in Fig. 5.

The collared coil is installed inside the vertically split yoke with 400 mm outer diameter made of SAE 1045 iron and fixed with Al clamps. The yoke length is 1950 mm which covers the entire coil and the Nb₃Sn/Nb-Ti lead splices. The 12 mm thick 304L stainless steel shell is pre-tensioned during welding to provide the coil final pre-compression. Two 50 mm thick 304L stainless steel end plates welded to the shell restrict the axial coil motion. Pictures of the collared coil assembly with iron yoke and the cold mass lead end are shown Fig. 6.



Fig. 6. Collared coil inside iron yoke (left) and cold mass lead end (right).

Magnet was heavily instrumented to monitor its parameters during assembly and test. Instrumentation includes 10 voltage taps (VT) on the inner layer and 9 VTs on the outer layer of each coil, 64 strain gauges (SG) on the coils, shell and end bullets, 4 resistive temperature sensors (RTD) along the magnet shell. Schematic of VT position is shown in Fig. 7.

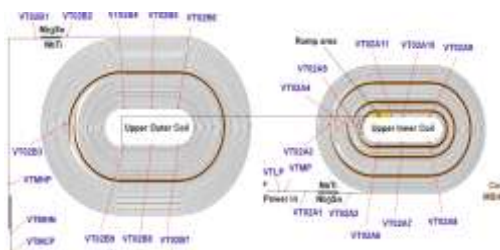


Fig. 7. Voltage tap position in inner and outer layers of coil.

IV. TEST RESULTS

Demonstrator dipole MBHSP01 was tested at FNAL Vertical Magnet Test Facility (VMTF). The test program included standard measurements of magnet quench training and ramp rate dependence both at 4.5 K and 1.9 K as well as temperature dependence, quench protection study and magnetic measurements.

Magnet quench history with quench location is shown in Fig. 8. Magnet training started at 4.6 K with the nominal current ramp rate of 20 A/s. The first quench was at ~8.8 kA originated in coil pole turn. However, after 5 quenches, originated in high field areas, magnet quench current was limited by quenches in outer-layer blocks of both coils. Quenching with lower ramp rates revealed that magnet quench current reduces with the ramp rate decrease. At ramp rates above 60 A/s the magnet ramp rate dependence had expected behaviour with quenches originated in the inner-layer midplane blocks. Similar behaviour was also observed at 1.9 K. After that magnet quenching was continued with different current ramp rates 40-70 A/s in order to reach the maximum possible quench current at both temperatures.

Ramp rate dependences of magnet quench current at 4.6 and 1.9 K are shown in Fig. 9. At both temperatures the magnet quench current reached its maximum at $dI/dt \sim 50-60$ A/s. No quench was detected when ramping down at 1.9 K from 8 kA at a ramp rate of 120 A/s. Short retraining was observed after the thermal cycle.

The maximum quench current at 4.6 K was 10.2 kA reached at $dI/dt = 60$ A/s. The absolute maximum of magnet quench current of 11.4 kA which corresponds to the magnetic field in aperture of 10.4 T was reached at 1.9 K at $dI/dt = 50$ A/s. The quench current limit for the demonstrator dipole was also estimated based on measured witness sample data. At 4.6 K it is 13.0 kA and at 1.9 K it is 15.0 kA which corresponds to the maximum bore field of 12.3 and 13.4 T respectively. The maximum reached field corresponds to 78% of SSL at $dI/dt = 0$.

The temperature dependences of the quench current expected based on SSL calculation and measured at a ramp rate of 50 A/s (in all quenches but one) are shown in Fig. 10. Magnet shows the normal temperature dependence of quench current, but exhibits its substantial degradation and some patterns of flux jump instability. All quenches at intermediate temperatures were initiated in the mid-plane block of coil 2 outer layer.

The observed limited quench performance could be caused by several reasons including J_c degradation and/or flux jumps in coil outer-layer leads. Bad splices could also explain the observed quench performance. Outer lead damage occurred during reaction of practice and spare coils. Possibilities of coil lead damage during magnet assembly are also not excluded.

To verify the above hypotheses several special tests and measurements were performed.

Fig. 11 shows quench current vs. holding time at current plateaux at 4.6 and 1.9 K. Magnet current was ramped to a pre-set current at 20 A/s and held until quench. Zero holding time is a regular quench at 4.5 K or 1.9 K at chosen ramp rate. All holding quenches initiated in the mid-plane block of coil 2

OL. Reproducibility test and tests at different ramp rates were not performed.

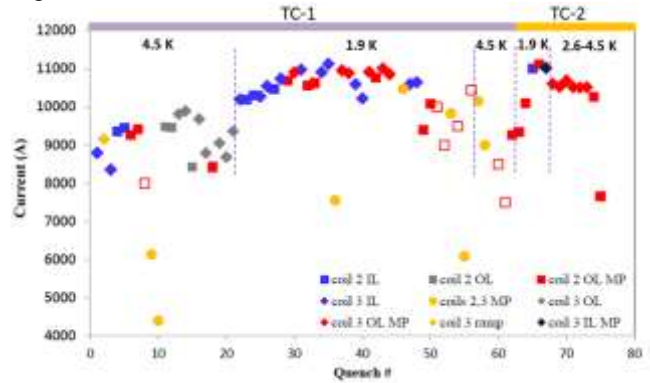


Fig. 8. Quench history and origin in TC1 and TC2.

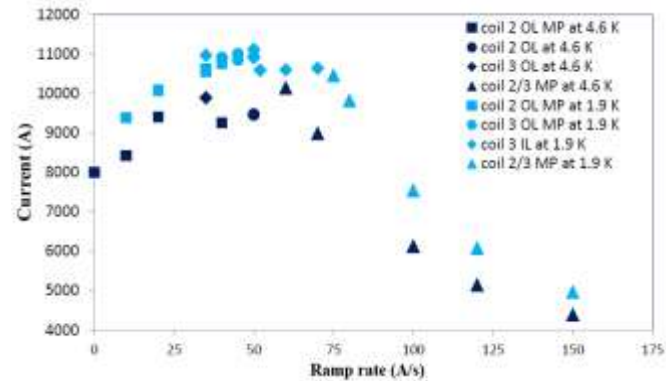


Fig. 9. Ramp rate dependence of magnet quench current at 4.6 and 1.9 K.

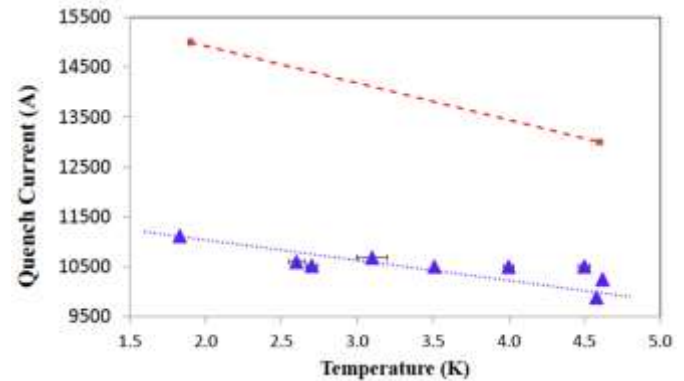


Fig. 10. Temperature dependence of magnet quench current ($dI/dt = 50$ A/s).

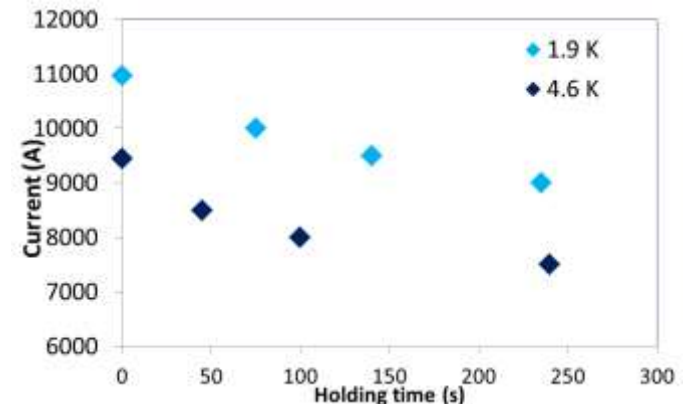


Fig. 11. Quench current vs. holding time at current plateaux at 4.6 and 1.9 K.

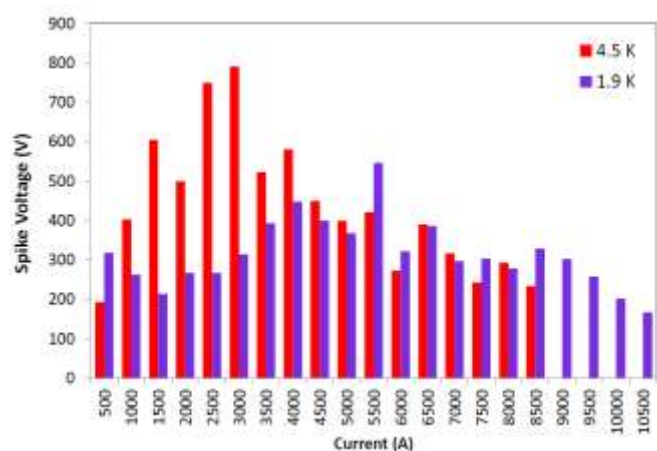


Fig. 12. Voltage spike distribution.

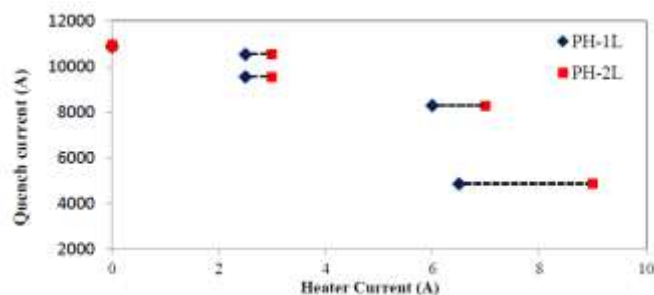


Fig. 13. Effect quench heaters on magnet quench current.



Fig. 14. RRR measurements in coil segments.

Analysis shows that stable current is 2.5 kA and 2 kA lower than quench current reached at 50 A/s at 1.9 and 4.6 K respectively which corresponds to currents extrapolated to $dI/dt=0$ on the ramp rate dependence shown in Fig. 9.

Fig. 12 shows voltage spike distribution during current ramp up recorded at 4.6 and 1.9 K. Comparing these data with the data collected for other Nb₃Sn magnets made of similar RRP-108/127 strand [10] one can conclude that their level is comparable and much lower than in magnets made of more unstable RRP-54/61 strand [11].

Special instability suppression test, similar to that described in [12] was performed by reducing J_c in the outer-layer mid-plane area by heating them with quench heaters powered with small DC current. No improvement of quench performance but quench current reduction was observed (see Fig. 13). This experiment as well as modest voltage spike activity do not support the idea that flux jumps are limiting the outer-layer quench current.

The residual resistivity ratio (RRR) of cable in coil was measured for all segments of both coils during magnet warming-up. RRR variation along the cable in coils is shown in Fig. 13. The average RRR value was ~ 100 (lowest 80, highest 118). One could notice that the same segments in different coils have similar RRR values. These numbers are smaller than ones measured in well-performed magnets made of the similar strand [10].

The splice resistances were also measured and found smaller than 2 nOhm.

V. CONCLUSION

The first 2 m long, single-aperture demonstrator dipole has been built and tested at FNAL. Magnet reached 10.4 T or 78 % of SSL at 1.9 K showing limited quench performance. Most quenches at low ramp rates, all holding quenches and quenches at intermediate temperatures initiated in the mid-plane block of the outer coil layer. Only few training quenches occurred in the high field area at the very beginning of test at 4.5 K and 1.9 K. Quench location, ramp rate and temperature dependence studies, and additional tests point out on the problems with coil outer-layer lead in both coils. Possible conductor damage in the mid-plane area during fabrication could cause the observed degradation. The investigation of all possible causes continues including magnet autopsy. All appropriate changes will be implemented in fabrication process of MBHSP02, a 1m long dipole model of the same design, and tested.

Experimental data related to magnet quench protection and field quality were also collected during this test providing an important input to magnet design and performance optimization.

Fabrication of two 2 m long collared coils for the first twin-aperture demonstrator dipole have started at FNAL.

ACKNOWLEDGMENT

The authors thank technical staff of FNAL Technical Division for contributions to magnet design and fabrication.

REFERENCES

- [1] L. Bottura et al., "Advanced Accelerator Magnets for Upgrading the LHC", *IEEE Trans. on Applied Supercond.*, accepted for publication, 2012.
- [2] A.V. Zlobin et al., "Development of Nb₃Sn 11 T Single Aperture Demonstrator Dipole for LHC Upgrades", *Proc. of PAC'2011*, NYC, 2011, p. 1460.
- [3] G. Chlachidze et al., "Quench heater study", ASC2012
- [4] N. Andreev et al., "Magnetic measurements", ASC2012
- [5] A.V. Zlobin et al., "Design and Fabrication of a Single-Aperture 11 T Nb₃Sn Dipole Model for LHC Upgrades", *IEEE Trans. on Applied Supercond.*, MT-22, 2012.
- [6] A.V. Zlobin et al., "IPAC2012.
- [7] M.B. Field et al., "Internal Tin Nb₃Sn Conductors for Particle Accelerator and Fusion Applications," *Adv. Cryo. Engr.*, vol. 54, 2008, p. 237.
- [8] E. Barzi et al., "Studies of Nb₃Sn Strands Based on the Restacked-Rod Process for High-field Accelerator Magnets", *IEEE Trans. on Applied Supercond.*, MT-12, 2012.
- [9] N. Andreev et al., "Volume expansion of Nb₃Sn strands and cables during heat treatment", *Adv. in Cryo. Engineer.*, V. 48, AIP, 2002, p. 941.

[10] LQM01,TQC03
[11] LQS01-02